Mapping Curie Point Depth of the West African Craton from Satellite Magnetic Data and its Implication for Diamond Exploration

A. Bouguern, K. Allek, M. Khalifa
Laboratory of Earth Physics, University of Boumerdes, Algeria
F. Bendiab
ENAGEO, Hassi Messaoud, Algeria
D. Boubaya
University of Tebessa, Algeria

ABSTRACT The main objective of this work is to map the Curie depth of the West African Craton (WAC) using satellite magnetic data with the aim to provide first order evaluation, within this vast territory, for the spatial association between Curie-depth surface and known kimberlite locations. Taking into account Clifford's rule, the first and foremost exploration guideline for diamond exploration is the existence of a sufficiently thick lithosphere that expected to have a low surface heat flow. The Curie depth is closely related to the surface heat-flow conditions and lithosphere thickness. In actual fact, the only few regions that have sufficient density of surface heat flow measurements corroborate the association of these conditions with the diamond resources. To better explore in an efficient way the spatial relationship between the Curie depth and known diamondiferous primary sources within the WAC, we used GIS-based weights of evidence method to provide a quantitative analysis.

1 INTRODUCTION

The diamonds form from carbon within the high-pressure environment present in nature at depths of over 150 km. In most parts of the Earth, at such depths we are right in the asthenosphere and the temperatures at this depth are too high to allow the crystallization of diamonds. However ancient cratonic blocks have a sufficiently thick (150-250 km) and relatively cool lithosphere (less than about 1200° C) in which diamonds can form and be preserved. The diamondiferous kimberlites are confined to these Precambrian cratons, particularly on those of Archean age. This empirical association is known as Clifford's rule (Clifford, 1966).

Thick and cool lithosphere potentially has a regional signature in almost all geophysical techniques. Teleseismic and magnetotelluric methods are the only methods able to directly "look" into the mantle. However, magnetic method may predict the presence of lithospheric root (thick lithosphere) rather than direct detection. Surface heat flow measurements may be the first predictive approach for identifying conditions favorable for primary diamond deposits, as temperature at depth is the primary controlling parameter in diamond genesis. Exploration targets for diamond genesis are expected to have a low heat flow of 40–45 mW m^{-2} (Morgan, 1995). Several studies have shown a strong correlation between heat flow measured at the surface and the thickness of the magnetized crust. As is known, crustal rocks lose their magnetization at the Curie point temperature (about 525 ± 25° C). At this temperature, ferromagnetic rocks become paramagnetic, and their ability to generate detectable magnetic anomalies disappears.

The depth to the Curie isotherm surface may be at mid-crustal levels in regions of high heat flow, and at or close to the Moho in stable, low heat-flow regions. Therefore, the maximum magnetic source-depth is closely related to the surface heat-flow conditions.

The objective of this study is to assess the spatial relationship between the mapped Curie depth, and the known kimberlites locations, to answer the question whether the spatial distribution of these kimberlites is controlled by Curie-depth in the WAC assumed to be closely related to Heat-flow conditions. A geospatial quantitative assessment based on Bayesian statistical approach, in a log-linear form know as Weights of Evidence modeling technique (Bonham-Carter, 1994), was used to quantitatively analyze the spatial association between the Curie-depth surface and kimberlites locations. This method has been applied previously by Paganilli et al (2002) to determine the spatial relationship of various direction lineaments to known kimberlite locations in the Canadian Buffalo Head Hills.

2 STUDY AREA AND DATA SETS

The vast extent (4.5 million km^2) Western African Craton (WAC) considered in this study covers many countries. It lies at the North-Western part of Africa, between 17°30' W - 3°30'E longitudes and 4°10'N - 30°40'N latitudes. The geological map of west Africa (Fig. 1) shows two shields of Precambrian rocks exposed in the Reguibat and Man uplifts, separated by the Taoudeni Basin. The southern Precambrian core covers most of Sierra Leone, Liberia and southeast Guinea. In this core are located the diamond-bearing kimberlites of Sierra Leone, Liberia and Guinea. The Reguibat shield is the northern core, almost the mirror image of the southern core. Kimberlite eruptions have been rare through geological ages with an important episode during Cretaceous times.

The basement of the WAC, stable since 2000 MA, is dominated by the occurrence of Archean nuclei surrounded by low-grade volcanoclastic Birrimian formations, which were affected by the Eburnean orogeny (at about 2 billion years) and intruded by numerous lower Proterozoic granitoids.

The data used in this study are extracted from satellite magnetic field model MF7 developed from CHAMP mission using measurements collected from May 2007 to April 2010. The original data set was compiled at 1.5 arc minute ascii grid of the anomaly of total intensity at 2.5 km altitude above the WGS84 ellipsoid. It is intended for use in the World Digital Magnetic Anomaly Map project for the 2011 revision. These data provide the most effective means of mapping the long wavelengths of the magnetic field caused by the magnetization of the Earth's crust. The CHAMP satellite, active until 2010, was launched in July 2000 into a lower orbit, initially at 450 km altitude. It has been providing excellent quality data at solar minimum conditions and at steadily decreasing altitudes. Using a field model instead of raw satellite magnetic field observations is highly productive as the magnetic field measured by a satellite contains contributions from several different sources: the core, the crust, the ionosphere, and the magnetosphere. Field modeling allows separation of various sources, thus allowing the crustal field to be isolated.

The crustal magnetic field of the WAC derived from world digital magnetic anomaly map was resample at a 4-km grid spacing resolution using Minimum Curvature interpolation method (Fig. 1). The main characteristics observable in the magnetic field are the NE-SW trends apparent in the central portion of the study area which seem affected by NW to WNW direction particularly in the northern part of the region. The most intense anomaly appears to be localized in the NE of Mauritania on the border with the Western Sahara. This large

sub-latitudinal bipolar anomaly present an amplitude of more than 500 nT, and most of the known kimberlite occurrences discovered in Mauritania are within this zone. To the southwestward termination, a magnetic low characterizes a E-W trend within a region on horseback between Guinea, Liberia and Sierra Leone, where all of the known diamond-bearing lithologies lie within this area.
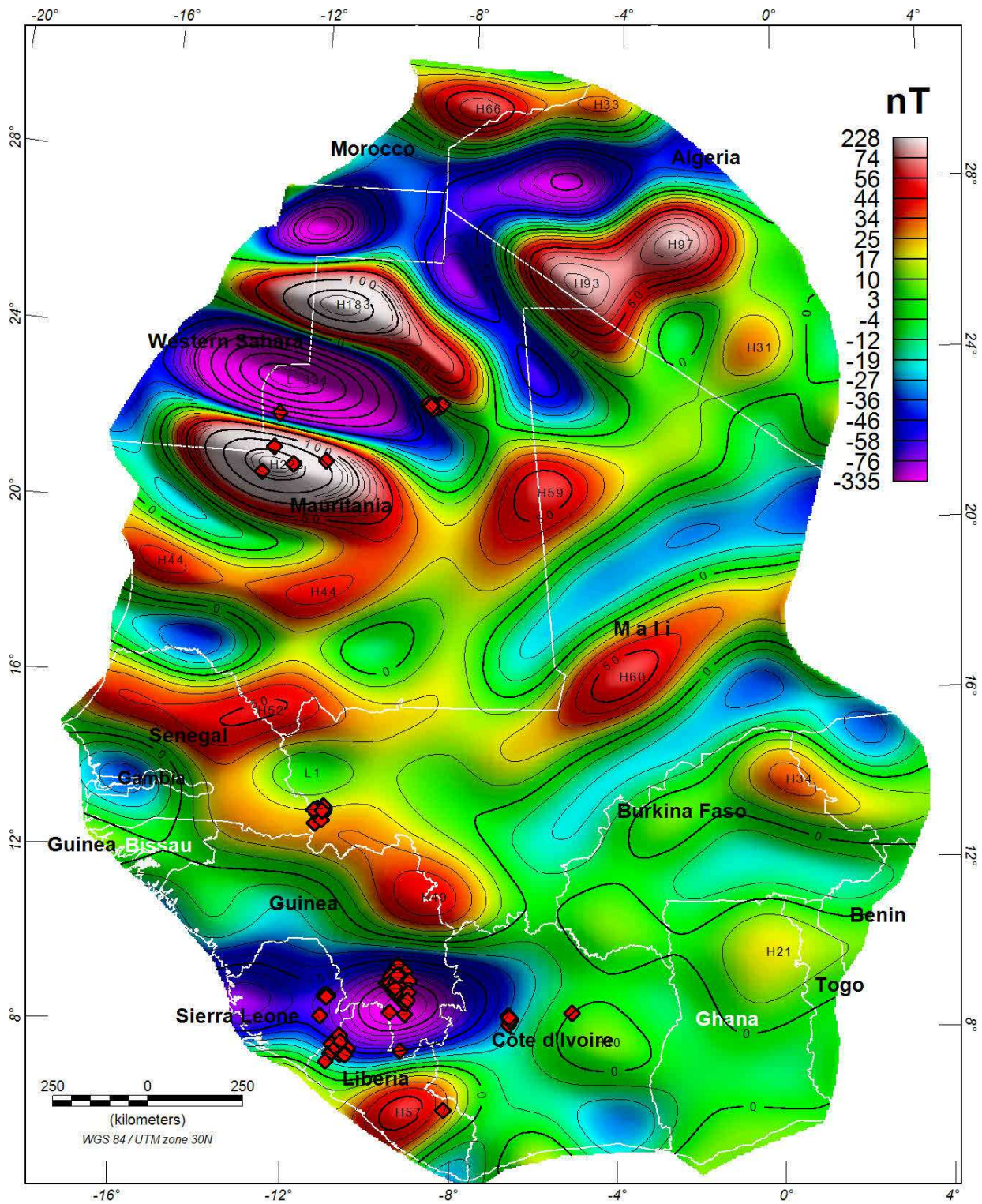

Figure 1: West African Craton crustal magnetic field and kimberlites locations

3 METHODOLOGY

3.1 Curie point depth estimation

The basic physical phenomenon that governs the investigation's of magnetic depth method is the Curie temperature by which the detection of magnetic bodies is limited by the depth of the Curie isotherm. Using magnetic data to infer heat flow is possible because the magnetic properties of rocks are temperature dependent, and at the Curie temperature rocks lose their magnetism. Negi *et al.* (1987) have elaborated empirical relationships which may be readily used in converting Curie depth into the corresponding surface heat flow density values and lithosphere thickness.

The geothermal heat flow is an important factor in the area selection for diamond exploration. The estimation of the depth to magnetic bottom, assumed to be at the Curie temperature, can be realized using spectral analysis. However, this approach depends upon many assumptions and therefore has limitations. It requires that the depth to the bottom of magnetic sources be large relative to the depth of the top, essential to spectral separation.

Magnetic data have been used in various parts of the world in order to estimate Curie Point Depths (CPDs). Two approaches have been usually used for the computation of the CPDs; the spectral peak and the centroid depths. The spectral peak approach originally is given by Spector and Grant (1970), and the centroid approach originally presented by Bhattacharyya and Leu (1977) and was developed by Okubo et al. (1985). As part of the work presented here, we used the first one.

Spector and Grant (1970) derived an expression for the power spectrum of the total magnetic field intensity by assuming that the anomalies are due to an ensemble of vertical prisms. The method treats the observed magnetic field anomalies as a statistical population. They demonstrated that contributions from the depth, width and thickness of a magnetic source ensemble could affect the shape of the energy spectrum.

The dominant term, which controls this shape, is depth factor. The depth estimates could be made using the equation,

$$E(r) = e^{-2hr} \qquad (1);$$

where E(r), h and r are the spectral energy, depth and frequency respectively. The thickness factor $(1 - e^{-tr})^2$ plays an interesting role in shaping the power spectrum. When combined with the depth factor (e^{-2hr}) (for not too large values of r), its effect is to produce a peak in the spectrum whose position shifts towards smaller wavenumbers with increasing values of $'t'$ (thickness). When this peak occurs (significant maximum), it indicates that the source bottoms are detectable. The frequency f_{max} of the spectral peak, the mean depth $'h'$ to the source tops (depth to deep-seated causative bodies) and the mean depth $'d'$ to the source bottom (Curie depth) are related by the equation (Boler 1978).

$$f_{max} = \frac{1}{2\pi(d-h)} ln\left(\frac{d}{h}\right) \qquad (2);$$

where d = h + t. Whether the sources appear to be depth limited or not depends very much on the size of the map. If there were no restrictions upon either the size of the map, then presumably the Curie-point depth isotherm could be observed. Therefore, large-scale magnetic maps are useful for understanding and characterization of crustal temperatures.

The WAC was subdivided in 209 square subregions (windows). The dimensions of these windows were initially set at 100 x 100 km²; in numerous cases this size was insufficient to allow the observation of spectral peak presumably related to the CPD because it occurs at frequency lower than the fundamental frequency for the subregion.

This led us to increase the size of the windows gradually by steps of 10 km until reaching a size of 150 x 150 km^2 which seems suitable for CPD determination.

The radially averaged power spectra were computed for each subregion. the Curie depth estimate is derived using equation (2). Graphs of the logarithms of the spectral energies against frequencies for the various blocks were obtained. Linear segment from the low frequency portion of the spectra, representing contributions from the deep-seated causative bodies could be drawn from each graph. The slope of the linear segment can be used to calculate the depth to the ensemble of causative bodies from the equation (1). An example of spectra for one subregion is given in Figure 2.
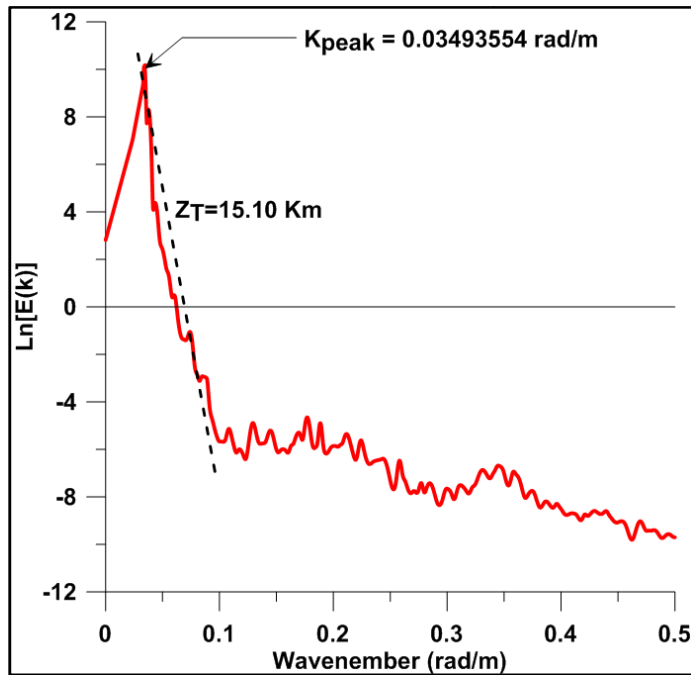

Figure 2: Example of spectrum for the estimation of the depth to Curie point using spectral peak approach.

The calculated Curie point depths were interpolated onto a regularly spaced grid using a minimum curvature technique (Briggs 1974). A grid with a cell size of 41 km was designed according to the known Rule applicable to data evenly distributed where the nominal cell size is = ¼ (sqrt (grid area / number of data points)). The data set

was resampled to a 4-km grid spacing resolution in order to have more precision in the location of favorable or unfavorable evidential zones (Fig. 3). Curie point depths (CPDs) of WAC vary between 18.5 and 51.5 km.

3.2 Weights of Evidence approach

Weights of evidence (*WofE*) is a Bayesian statistical method for assessing the degree of spatial association and for combining evidence to test a hypothesis. It determines the probability of an event to occur under certain conditions. The method was originally developed for a non-spatial application in medical diagnosis, later it was extensively used for mineral potential mapping in a GIS environment (Bonham-Carter, 1994), and soon after adapted for landslide susceptibility analysis, hazard modeling, fires and so on. The WofE method is applied here to investigate the spatial associations between Curie point depths and known kimberlite occurences within the WAC. The importance of the weights depends on the measured association and permits to provide an insight into the thermal flow condition of the WAC. This method could be used as spatial evidence in diamond prospectivity mapping.

A detailed explanation of the mathematical formulation of the WofE modeling method is available in Bonham-Carter (1994). The method uses a log-linear of the Bayesian probability model to estimate the importance of evidences by a pair of weights, one (positive weight W^+) for presence of the evidence H, and negative weight (W^-) for absence of the evidence H.

$$W^+ = ln\left(\frac{P(C|K)}{P(C|\bar{K})}\right) \qquad (3)$$

$$W^- = ln\left(\frac{P(\bar{C}|K)}{P(\bar{C}|\bar{K})}\right) \qquad (4)$$

where P() denotes probability, C is the presence of predictive pattern (it corresponds to area occupied by class of CPDs), $\bar{C}$ is the absence of predictive pattern, K is the presence of training points of interest
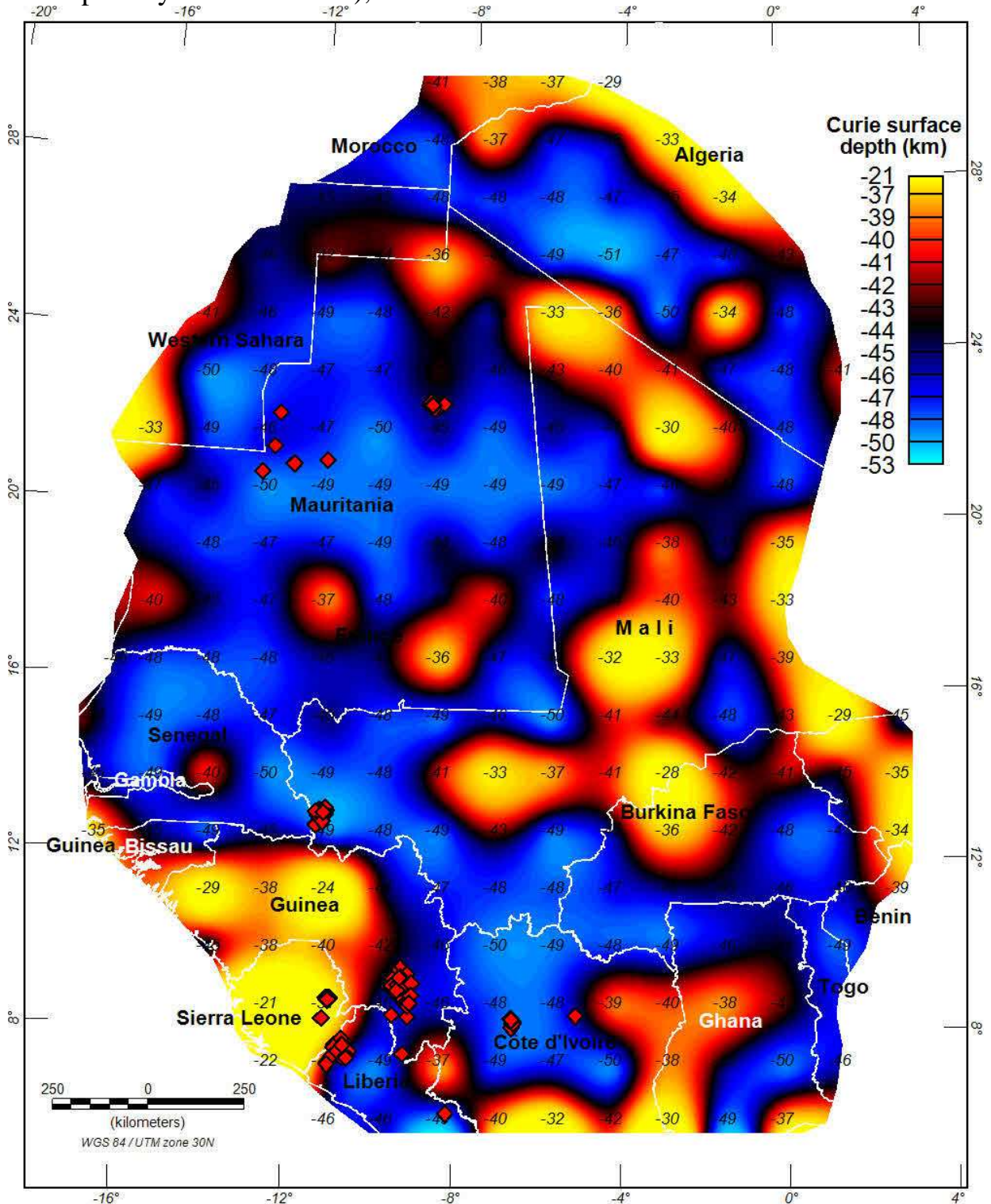

Figure 3: Curie-point isotherm map of the study area and kimberlite locations. CPDs of each subregion are reported on the map

corresponds to kimberlite occurrences), $\bar{K}$ is the absence of kimberlite occurrence.

The weights (W^+ and W) provide a measure of spatial association between the training points K and the binary theme C.

The value of the weight W^+ is positive, whereas W is negative, indicates that there are more kimberlite occurrences on theme class C than would occur due to chance. Conversely W^+ would be negative and W

positive for the case where fewer points occur than expected. If the kimberlite occurrences K are distributed randomly with respect to the binary theme C, then both of weights will have a value of zero, or very close to zero. The difference between the weights is known as the contrast, C. Thus:

$$C = W^+ - W^- \qquad (5)$$

The contrast is an overall measure of spatial association between the set of points K and the theme C, combining the effects of the two weights. It is the best estimator in a large area and when a large number of points occurrences are considered (Bonham-Carter, 1994). Hence, for a positive correlation, C is positive; C is negative in the case of negative spatial correlation.

The studentized confidence value *s(C)*, defined as the contrast *C* divided by its standard deviation, corresponds approximately to the statistical level of significance defined by standard z-tests, and provides a useful measure of the significance of the contrast (Raines, 1999). The standard deviation of C is calculated as:

$$s(C) = \sqrt{s^2(W^+) + s^2(W^-)} \qquad (6)$$

In the spatial analysis, as applied in this work, a simplified and intuitive approach similar to that suggested by Turner (1997), was adopted. The surface of the study area and the predictive pattern C are expressed in number of unit cells, and each training point is assumed to occupy a single unit cell. That way, the weights W^+ and W^- can be calculated by means of map crossing functions as follows:

$$W^+ = \ln\left(\frac{\dfrac{Number\ of\ training\ points\ K\ (kimberlites)\ \textbf{inside}\ the\ pattern\ C}{Total\ number\ of\ points\ K}}{\dfrac{Number\ of\ unit\ cells\ \textbf{inside}\ pattern\ C\ not\ occupied\ by\ points\ K}{Total\ number\ of\ unit\ cells\ of\ the\ study\ area\ not\ occupied\ by\ points\ K}} \right) \qquad (7)$$

$$W^- = \ln\left(\frac{\dfrac{Number\ of\ training\ points\ K\ \textbf{outside}\ the\ pattern\ C}{Total\ number\ of\ points\ K}}{\dfrac{Number\ of\ unit\ cells\ \textbf{outside}\ pattern\ C\ not\ occupied\ by\ points\ K}{Total\ number\ of\ unit\ cells\ of\ the\ study\ area\ not\ occupied\ by\ points\ K}} \right) \qquad (8)$$

A unit cell of 4 km x 4 km was used. The total number of unit cells area (16 km²) in the study area map is 289 181 cells. The training points used for the spatial association analysis are all diamond-bearing lithologies, namely: mafic lamprophyres, lamproites, and kimberlites from Côte d'Ivoire, Guinea, Mali, Sierra Leone, Liberia, and Mauritania publically available from World kimberlites CONSOREM database (Faure 2010).

4 SPATIAL ASSOCIATION ANALYSIS

The locations of 141 known diamondiferous primary sources (mainly kimberlites) have been used as training points to quantitatively analyze the spatial association with Curie point depths. Each

training point/kimberlite is assumed to occupy a small unit area, defining the 'unit cell area'. Given that some kimberlite occurrences are very close to each other, we used a systematic reduction in the number of training points by geographic *weeding* - removing training points that are too close together. The minimum spacing is taken as the unit cell size specified when defining the study area, i.e. 4 km. After removing the undesirable items, we lead to 109 training points.

A multiclass Curie Point Depths (CPDs) map was produced from the reclassification of the original continuous grid into ten classes to create the Curie surface depth theme as shown in Figure 4. This multiclass

predictor theme provides a representation of heat flow conditions in relation to kimberlite occurrences. For the weights calculations, we have initially calculated the weights for each class (table 1). Because some of the classes may have a very small number of kimberlite occurring in them and this is particularly critical for the weights calculated in this case, we experiment the computation of weights for cumulative Curie point depths, and to examine the variation of the weights and contrast at successive cumulative CPDs intervals (Table 2)

The relative weights and contrasts values of the CPDs theme are shown in Table 1 and 2. As indicated by contrasts C, they clearly outline a strong spatial correlation with CPDs class interval (53 to 49 km) in which 19 kimberlite occurrences are present. A less important spatial correlation seems to be present with the CPDs class (46 to 43 km), despite the occurrence of 49 kimberlite occurrences, resulting from the large area units proportion covered by this Curie depth class, with respect to the number of kimberlite occurrences. This spatial association between kimberlite occurrences and deepest Curie-points is due to the role of low heat flow as the primary controlling parameter in diamond genesis. This result is supported by some studies have shown a strong correlation between heat flow measured at the surface and the thickness of the magnetized crust.

which reveals favourable lithospheric conditions

In general the surface heat flow reflects the tectonic stabilization of the crust, i.e. the stable old structures are characterized by low heat flow, and the young geologically active areas presumably have to display relatively high Moho heat flow. It can be concluded, from Figs. 12 and 13, that the heat flow decreases with an increase in Curie depth, as suggested by Negi et al. (1987).
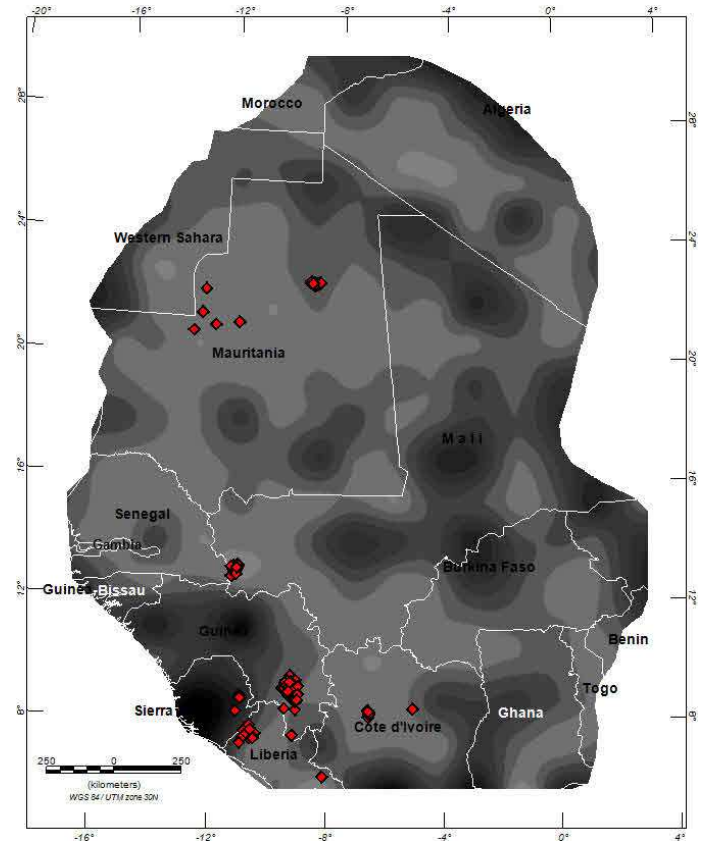

Figure 4: Classified Curie point depths map and kimberlite locations

Table1: Summary of weights for each class of CPDs

Class CPD (km)	Area (km²)	Area (units)	No. Points	W+	W-	Contrast	Confidence
-53 to -49	45600	2850	19	2.858	-0.181	3.040	12.006
-49 to -46	1704976	106561	20	0.718	0.269	-0.988	-3.991
-46 to -43	1262768	78923	49	0.478	-0.270	0.749	3.888
-43 to -40	694816	43426	13	0.251	0.039	-0.291	-0.984
-40 to -37	450288	28143	0				
-37 to -33	226592	14162	0				
-33 to -30	95760	5985	8	1.246	-0.055	1.301	3.539
-30 to -27	21520	1345	0				
-27 to -24	12752	797	0				
-24 to -20	16048	1003	0				

Table 2: Summary of weights for cumulative classes of CPDs

Class CPD (km)	Area (km²)	Area (units)	No. Points	W+	W-	Contrast	Confidence
-53 to -49	45600	2850	19	2.858	-0.181	3.040	12.006
-49 to -46	1750576	109411	39	0.077	0.045	-0.122	-0.612
-46 to -43	3013344	188334	88	0.194	-0.553	0.747	3.077
-43 to -40	3708160	231760	101	0.124	-0.906	1.031	2.806
-40 to -37	4158448	259903	101	0.010	-0.114	0.124	0.337
-37 to -33	4385040	274065	101	0.043	0.823	-0.866	-2.357
-33 to -30	4480800	280050	109	0.011	0.000	0.011	0.000
-30 to -27	4502320	281395	109				
-27 to -24	4515072	282192	109				
-24 to -20	4531120	283195	109				

5 CONCLUSION

Although the formulation of a kimberlite prospectivity mapping is not the objective of this study, the spatial association between kimberlite occurrences and deepest Curie-points is of potential importance for diamond exploration, as it may enable us to predict the diamond potential of target areas within craton on the basis of the mapped Curie point isotherm.

After these quantifications of spatial analysis, it could be implied that zones of deepest Curie-points can be fertile for diamond-bearing lithologies emplacements. This condition is most commonly found in regions of thick and cold lithosphere, and are consistent with Clifford's Rule, an empirical diamond exploration strategy.

REFERENCES

Bhattacharyya, B.K., Leu, L.K., 1977. Spectral analysis of gravity and magnetic anomalies due to rectangular prismatic bodies. *Geophysics 42, 41–50.*

Boler, F. M., 1978. Aeromagnetic measurements, magnetic source depths and the curie point isotherm in the Vale-Owyhee, Oregon, *M.Sc thesis, Oregon State University, Corvallis.*

Bonham-Carter, G.F., 1994. Geographic Information Systems for Geoscientists; Modelling with GIS *Pergamon. United Kingdom, 398 p.*

Briggs, I.C., 1974. Machine contouring using minimum curvature. *Geophysics 39, 39–48.*

Clifford, T.N., 1966. Tectono-metallogenic units and metallogenic provinces of Africa. *Earth Planet. Sci. Lett. 1, 421–434.*

Faure, S, 2010, World Kimberlites Database (Version 3), *Consortium de Recherche en Exploration Minérale CONSOREM, Université du Québec à Montréal, Numerical Database on www,consorem,ca,*

Hojat A., Guya N. H.,, and Maule C. F., 2010. A new method to determine geothermal potential sites using satellite magnetic field models, *Iranian Journal of Geophysics, 4 (1) 33-43.*

Mayhew, M.A., 1985. Curie isotherm surfaces inferred from high-altitude magnetic anomaly data. *J. Geophys. Res. 90 (B3), 2647–2654.*

Morgan, P., 1995. Diamond exploration from bottom up: regional geophysical signatures of lithosphere conditions favourable for diamond exploration. *J.Geochem.Explor. 53, 145–165.*

Negi, J.G., Agrawal, P.K., Pandey, O.P., 1987. Large variation of curie depth and lithospheric thickness beneath the Indian Subcontinent and a case for magnetothermometry. *Geophys. J. R. Astr. Soc. 88, 763–775.*

Okubo, Y., Graf, R.J., Hansen, R.O., Ogawa, K., Tsu, H., 1985. Curie point depths of the island of Kyushu and surrounding areas, Japan. *Geophysics 50, 481–494.*

Raines, G.L., 1999. Evaluation of weights of evidence to predict epithermal-gold deposits in the great basin of the Western United States. *Natural Resources Research 8, 257–276*

Spector A., and Grant F. S. 1970, Statistical Models for Interpreting Aeromagnetic Data, *Geophysics. 35, 293–302.*